BIOCHEMISTRY
including biophysical chemistry & molecular biology

Article

pubs.acs.org/biochemistry

Identification of Formation of Initial Native Structure in Onconase from an Unfolded State

Robert F. Gahl,[†] Robert E. Oswald,[‡] and Harold A. Scheraga*,[†]

[†]Baker Laboratory of Chemistry, Cornell University, Ithaca, New York 14853-1301, United States

[‡]Department of Molecular Medicine, Veterinary Medical Center, Cornell University, Ithaca, New York 14853-6401, United States

ABSTRACT: In the oxidative folding of onconase, the stabilization of intermediates early in the folding process gives rise to efficient formation of its biologically active form. To identify the residues responsible for the initial formation of structured intermediates, the transition from an ensemble of unstructured three-disulfide species, $3S_U$, to a single structured three-disulfide intermediate species, des-[30−75] or $3S_F$, at pH 8.0 and 25 °C was examined. This transition was first monitored by far-UV circular dichroism spectroscopy at pH 8.0 and 25 °C, showing that it occurs with the formation of secondary structure, presumably because of native interactions. The time dependence of formation of nativelike structure was then followed by nuclear magnetic resonance spectroscopy after we had arrested the transition at different times by lowering the pH to 3 and then acquiring $^{1}H-^{15}N$ heteronuclear single-quantum coherence spectra at pH 3 and 16 °C to identify amide hydrogens that become part of nativelike structure. H/D exchange was utilized to reduce the intensity of resonances from backbone amide hydrogens not involved in structure, without allowing exchange of backbone amide hydrogens involved in initial structure. Six hydrogen-bonding residues, namely, Tyr38, Lys49, Ser82, Cys90, Glu91, and Ala94, were identified as being involved in the earliest detectable nativelike structure before complete formation of des-[30−75] and are further stabilized later in the formation of this intermediate through S−S/SH interchange. By observing the stabilization of the structures of these residues by their neighboring residues, we have identified the initial, nativelike structural elements formed in this transition, providing details of the initial events in the oxidative folding of onconase.

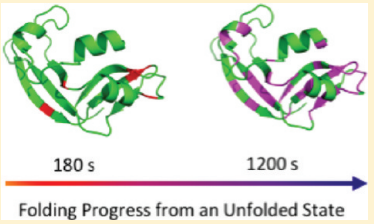

Previous investigations of the oxidative folding pathways of disulfide-bond-containing proteins have shown that the rate of recovery of the biologically active forms of these proteins from a reduced state containing no disulfide bonds is very slow compared to the rate of recovery of these native structures when their disulfide bonds are intact.[1,2] Therefore, the oxidative folding process can be stopped at various times and analyzed to extract kinetic and thermodynamic information about intermediate species formed along the folding pathways. This study takes advantage of the ability to arrest disulfide bond-dependent folding to determine the initial structure(s) formed during the recovery of native onconase (ONC) (Figure 1). In previous studies,[3−9] hydrogen/deuterium exchange, monitored by NMR or mass spectroscopy, was used to analyze different stages of the folding process. In this study, NMR spectroscopy is used to determine the initial nativelike structure(s) during disulfide bond-dependent folding.

Onconase is a 104-residue, four-disulfide homologue of bovine pancreatic ribonuclease A (RNase A). The following mechanism has been proposed for the oxidative folding of ONC:[2] where R is an ensemble of reduced onconase species, nS_U is an unstructured ensemble that contains n mostly non-native disulfide bonds, and des-[x−y,...] is a structured species with native disulfide bonds but lacking the [x−y,...] disulfide bond(s). The oxidative folding pathway, starting from R, begins with an oxidation to form the unstructured $1S_U$ ensemble. This $1S_U$ ensemble can be oxidized to produce the structured, two-disulfide species, des-[19−68, 30−75], or the unstructured $2S_U$ ensemble in another pre-equilibrium. Des-[19−68, 30−75] can be oxidized to either

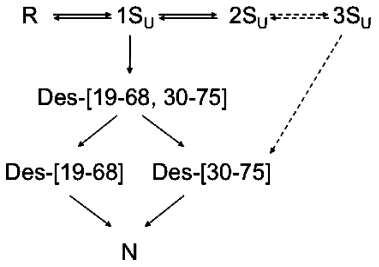

(1)

des-[19−68] or des-[30−75], each of which can be oxidized to the native 104-residue form (N). Des-[19−68] can also be obtained by oxidation of the $2S_U$ ensemble (not shown). Of the pathways from the $1S_U$ ensemble, the oxidation to form des-[19−68, 30−75] is more favored than the oxidation to the $2S_U$ ensemble. Because of the resulting weak production of $2S_U$, no further oxidation to form the unstructured $3S_U$ ensemble from the $2S_U$ ensemble is observed in the oxidative folding pathway under a range of oxidation conditions.[2] However, if folding were *initiated* from the unstructured $3S_U$ ensemble, four structured species, $3S_F$, namely, des-[19−68], des-[30−75], des-[48−90], and des-[87−104], could potentially be produced by S−S/SH interchange in the absence of an oxidizing or reducing agent. However, in the transition from $3S_U$ to $3S_F$ for ONC, only one

Received: July 28, 2011
Revised: November 19, 2011
Published: December 5, 2011

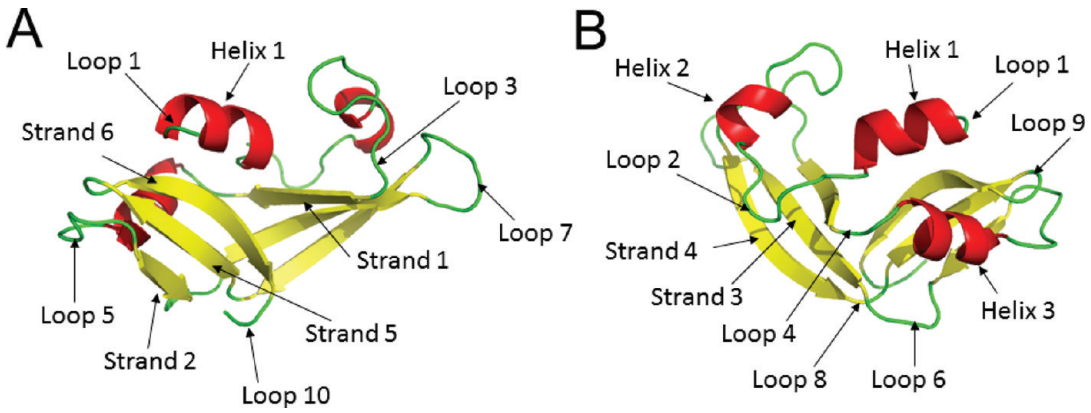

Figure 1. X-ray structure of ONC (PDB entry 1ONC). Panels A and B are two views of ONC that show numbered helices (red), strands (yellow), and loops (green).

structured species, des-[30−75], is observed, presumably because it is the most thermodynamically favorable one of the four. This intermediate had been identified from previous work,[10] and the formation of des-[30−75] has been observed previously.[11]

The goal of this investigation was to identify the region of onconase in which structure is formed, initially, in the passage from the $3S_U$ ensemble to a single $3S_F$ species, des-[30−75]. NMR spectroscopy was used to investigate the stepwise formation of nativelike structure in the $3S_U$-to-$3S_F$ transition in onconase, by starting with a $3S_U$ ensemble. A sample of $3S_U$ was prepared by reducing native ONC to obtain a maximal amount of only the des-[30−75] species, purifying it, and reshuffling it in the presence of GdnHCl to a $3S_U$ ensemble by S−S/SH interchange. The progress of the $3S_U$-to-$3S_F$ transition was followed by reducing the disulfide bonds of unstructured species but not the disulfide bonds of the structured des-[30−75] product. The increase in the concentration of des-[30−75] from the $3S_U$ ensemble is driven by formation of nativelike structure and is demonstrated here by the formation of nativelike far-UV CD spectra that accompany the increase in the concentration of des-[30−75], as well as by the appearance of resonances in $^{15}N-^{1}H$ HSQC spectra that correspond to those of native ONC as this transition proceeds. In addition, S−S/SH reshuffling in this transition was stopped at given times by lowering the pH to take advantage of the fact that the reactive species in S−S/SH reshuffling is the thiolate ion, whose concentration can be reduced at low pH by ∼5 orders of magnitude by converting the thiolate ions to thiols. By stopping the folding progress before completion in this manner, the system can be analyzed by NMR spectroscopy ($^{1}H-^{15}N$ HSQC). The goal of this investigation is to use NMR to identify the residues responsible for the initial formation of nativelike structure in the $3S_F$ oxidative folding intermediate, des-[30−75], from an unfolded state ($3S_U$).

MATERIALS AND METHODS

Materials. The plasmid for frog ONC was provided by R. J. Youle and used in the ^{15}N-enriched expression of ONC with the same protocol used previously.[12] As in those methods, 97% enrichment was attained as determined by mass spectroscopy.

Stable isotopes ([^{15}N]ammonium sulfate, d_4-acetic acid, and D_2O) were purchased from Cambridge Isotopes. All other reagents, including Tris, acetic acid, and GdnHCl, were purchased from Sigma-Aldrich and Fisher and used without further purification.

Shigemi tubes were used for the NMR experiments, and Millipore concentrators [3000 molecular weight cutoff (MWCO)] were used to concentrate the samples for use in the NMR experiments.

Preparation of the $3S_U$ Ensemble of ^{15}N-Enriched ONC. A $3S_U$ ensemble was generated from des-[30−75], which was obtained by reductive unfolding of ^{15}N-enriched ONC,[13] and purified by chromatography as shown below. The disulfide bonds of des-[30−75] were then reshuffled by S−S/SH interchange under denaturing conditions [7 M GdnHCl (pH 8.3)] to produce an ensemble of unfolded structures ($3S_U$) with mostly non-native disulfide bonds without any native conformations.

In the reductive unfolding pathway,[13] native onconase is reduced to the three-disulfide-bond-containing species, des-[30−75], which is further reduced to R. To maximize the amount of des-[30−75] produced by limited reduction, native ONC at 1 mg/mL was incubated in a pH 8.0, 0.1 M Tris buffer containing 10 mM DTT^{red}. After 2 h, the reductive unfolding of ONC was stopped via addition of glacial acetic acid. Des-[30−75] was purified by isolation from the reductive unfolding mixture by RP-HPLC using a water/acetonitrile buffer system with 0.09% TFA and a 25 cm × 4.6 mm SULPELCO Discovery BIO Wide Pore C18, 5 μm particle size column with the eluting species monitored by absorbance at 210 nm. After the reductive unfolding mixture was loaded onto the column, a constant flow of 85% water and 15% acetonitrile eluted the Tris and DTT^{red}. Then, a gradient of 30 to 45% acetonitrile over 60 min was sufficient to separate des-[30−75] from native ONC.[10] After des-[30−75] was collected, it was frozen, and then the TFA, water, and acetonitrile were removed by lyophilization. The lyophilized protein was reconstituted in a pH 3, 50 mM acetate buffer and stored at −70 °C until further use.

To generate the $3S_U$ ensemble by S−S/SH reshuffling, the solution containing the des-[30−75] species at a protein concentration of 0.5 mg/mL was incubated in a pH 8.3, 0.1 M Tris buffer that contained 7 M GdnHCl that had been previously purged of dissolved oxygen by humidified argon. The S−S/SH reshuffling was allowed to proceed for 2 h and stopped by addition of glacial acetic acid to lower the pH to 3. Buffer salts and GdnHCl were removed with a G25 size-exclusion column with a pH 3, 50 mM acetic acid buffer as the running buffer, and the eluting species were monitored at 280 nm. The desalted $3S_U$ ensemble was collected and frozen. Water and acetic acid were removed by lyophilization, and the $3S_U$ ensemble was reconstituted in 50 mM acetic acid at a concentration of 5 mg/mL.

dx.doi.org/10.1021/bi201168d | *Biochemistry* 2012, 51, 521−532

A DTT^{red} reduction pulse was applied to an aliquot of the solution of the $3S_U$ ensemble to reduce any non-native disulfide bonds in the aliquot because there was no structure present to protect the disulfide bonds from reduction. A far-UV CD spectrum of the solution showed that no secondary structure was present (data not shown).

Monitoring the $3S_U$-to-$3S_F$ Transition of ONC by Far-UV CD Spectroscopy and RP-HPLC. The $3S_U$-to-$3S_F$ transition was then initiated by incubating the $3S_U$ ensemble under folding conditions that allow S−S/SH exchange to lead to the structured species, des-[30−75] preferentially. Far-UV CD spectroscopy was used initially to detect the formation of structure during the $3S_U$-to-$3S_F$ transition that could then be followed by NMR spectroscopy. To initiate the $3S_U$-to-$3S_F$ transition for the far-UV CD spectroscopic experiments, an aliquot of the $3S_U$ stock solution was diluted to a final protein concentration of 0.2 mg/mL in a pH 8.0, 10 mM phosphate buffer (folding conditions) that was previously purged of dissolved oxygen using humidified argon. The mixture was transferred to a cuvette, which was then capped and sealed with parafilm, and the CD signal was monitored for folding at 205 nm for 30 min. A dead time of ~2 min between the preparation of the cuvette and the initial readings was incurred. An analysis by RP-HPLC of the final products showed the absence of oxidation during the transition; only S−S/SH interchange occurred in this 30 min period.

As a control, the MRE values of unfolded and folded protein during the same time period were obtained. The unfolded signal was obtained by diluting the $3S_U$ stock into pH 3, 50 mM acetic acid buffer to a final concentration of 0.35 mg/mL. Because there is no S−S/SH reshuffling at pH 3, no progress in the $3S_U$-to-$3S_F$ transition can occur. For the folded signal, a sample of des-[30−75] was diluted into the same pH 3 buffer to a final concentration of 0.25 mg/mL. The pH of 3 was chosen to avoid S−S/SH reshuffling by thiolates, which are present at a very low concentration at this pH. At different times, the MRE signal at 205 nm of these two samples was averaged for 2 s, and the average and standard deviation during this time were acquired.

In addition to monitoring the formation of secondary structure in this transition by CD, we also measured the distribution of $3S_U$ and $3S_F$ by RP-HPLC. To initiate the transition, an aliquot from the same 5 mg/mL stock solution of $3S_U$ was diluted to a final protein concentration of 0.2 mg/mL in a pH 8.0, 100 mM Tris buffer that was previously purged of dissolved oxygen using humidified argon. At different times, an aliquot from this mixture was removed and subjected to 5 mM DTT^{red} for 2 min. Under these conditions, the disulfide bonds of unstructured species are reduced but the disulfide bonds of des-[30−75] are not reduced because of the protection of these bonds by the presence of structure in this species. The reduction was then quenched by addition of glacial acetic acid. Samples were immediately frozen at −70 °C prior to analysis by RP-HPLC. The des-[30−75] was separated from other $3S_U$ species by RP-HPLC as described in the previous section. The results from the CD experiments and RP-HPLC analysis provided a basis for the time scale to use in the NMR experiments.

Acquisition of the NMR Spectrum of Native [^{15}N]ONC (N-ONC) at 16 °C and pH 3. Varian 500 and 600 MHz NMR spectrometers were used to record ^{1}H−^{15}N HSQC spectra at 16 °C and pH 3. Previous assignments of the ^{1}H and ^{15}N resonances of N-ONC had been acquired at 37 °C and pH 3.[14] Three-dimensional (3D) ^{15}N NOESY-HSQC and 3D ^{15}N TOCSY-HSQC NMR spectra of a sample of N-ONC were recorded at 37 °C and pH 3, prepared by using the procedure outlined in Figure 2A, to confirm previous assignments in ^{1}H−^{15}N HSQC spectra under these conditions.

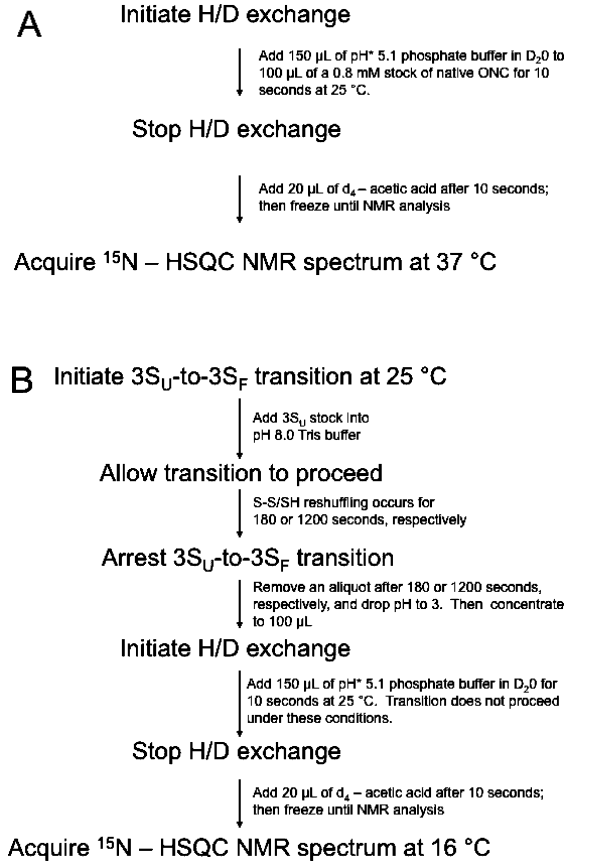

Figure 2. (A) Procedure for obtaining the ^{15}N HSQC NMR spectrum of native ONC at 37 °C. (B) Procedure for following the $3S_U$-to-$3S_F$ transition by NMR at 16 °C for 180 and 1200 s. H/D exchange reduced the intensity of the peaks arising from unfolded resonances without affecting those from structured residues.

To obtain these assignments at 16 °C and pH 3, where the ^{1}H−^{15}N HSQC spectra of acid-arrested $3S_U$-to-$3S_F$ transition aliquots were acquired, the spectra of N-ONC were recorded in 3−4 °C decrements from 37 to 16 °C at pH 3 over a total time of 20 min for each spectrum. By following the continuous change in the positions of the peaks as the temperature was varied, we assigned 91 of the 97 previously assigned resonances[14] observed in the ^{1}H−^{15}N HSQC spectrum at 16 °C. These assignments were used to identify structure-stabilized resonances along the $3S_U$-to-$3S_F$ pathway.

When these spectra were acquired at different temperatures, N-ONC was subjected to the same solvent conditions that were used later for the aliquots of the solution undergoing the $3S_U$-to-$3S_F$ transition, as outlined in Figure 2. A 100 μL aliquot of a 0.8 mM stock of N-ONC added to a 150 μL aliquot of a pH* 5.1, 50 mM phosphate buffer in D_2O, and hydrogen/deuterium exchange was allowed to proceed for 10 s at 25 °C and pH* 5.1 to decrease the intensity of cross-peaks from unfolded regions yet maintain those from folded regions. After 10 s, the pH* of each of the exchanged solutions was lowered to 3 with d_4-glacial acetic acid and each sample immediately frozen until it could be analyzed by NMR.

Acquisition of NMR Spectra during the $3S_U$-to-$3S_F$ Transition of ^{15}N-Enriched ONC. The protocol for analyzing the $3S_U$-to-$3S_F$ transition of ^{15}N-enriched ONC at different times is shown in Figure 2B. The $3S_U$-to-$3S_F$ transition was initiated by adding an aliquot of the $3S_U$ stock to an oxygen-purged solution of 0.1 M Tris (pH 8.0) in H_2O to a final volume of 3.4 mL and a final protein concentration of 0.2 mg/mL. After the $3S_U$-to-$3S_F$ transition was allowed to proceed for 180 s, half of the reaction mixture was removed, and the pH of this half was lowered to 3 by addition of 200 μL of glacial acetic acid and immediately put on ice. After 1200 s, to allow for the complete formation of $3S_F$, 200 μL of glacial acetic acid was added to the other half of the reaction mixture and that half immediately placed on ice. Using 3000 MWCO Millipore concentrators, the two aliquots were concentrated to a final volume of 100 μL at 4 °C. Each aliquot was subjected to hydrogen/deuterium exchange for 10 s at 25 °C as described in the previous section. The hydrogen/deuterium exchange time of 10 s is less than 1% of 1200 s, the time required to complete the $3S_U$-to-$3S_F$ transition, and therefore, it was assumed that there was no progress in the $3S_U$-to-$3S_F$ transition during the hydrogen/deuterium exchange time. The protein concentration of each of the samples for the NMR experiments was 100 μM. The total time to obtain the spectrum of each aliquot of the $3S_U$-to-$3S_F$ transition solution at 16 °C and pH 3 was 5.5 h. For a control sample, in which no folding was allowed to proceed, 150 μL of the pH* 5.1, 50 mM phosphate buffer in D_2O was added directly to a 100 μL aliquot of the 5 mg/mL stock of the $3S_U$ ensemble, which was not exposed to pH 8.0, and H/D exchange was allowed to occur before analysis by NMR.

By lowering the pH of aliquots taken 180 and 1200 s into the $3S_U$-to-$3S_F$ transition to 3, we arrested the progress of the transition. A control experiment, letting the aliquot taken 180 s into the $3S_U$-to-$3S_F$ transition remain under these low-pH arrested conditions at 16 °C for a longer time, showed that no progress in this folding transition was observed at this pH and temperature for 22 h. During this time, no increase in the amount of $3S_F$ or air oxidation was observed via examination of the distribution of species by RP-HPLC.

RESULTS

CD Spectra of the $3S_U$-to-$3S_F$ Transition of ^{15}N-Enriched ONC. Analysis of the $3S_U$-to-$3S_F$ transition by RP-HPLC shows that des-[30−75], a nativelike oxidative folding intermediate,[2,10,11] is preferentially populated as the transition proceeds. In Figure 3A, unstructured species dominate 360 s into the transition. However, in panels B and C of Figure 3, the structured intermediate, des-[30−75], dominates the distribution at 1040 and 1800 s. The identical ratio of des-[30−75] to unstructured species at 1040 and 1800 s suggests that the distribution of three-disulfide-bonded species has attained equilibrium. No des-[30−75] is observed after 1800 s when 3.5 M GdnHCl is present before initiation of the $3S_U$-to-$3S_F$ transition (Figure 3D). Analyzing this transition by far-UV CD spectra shows that the increase in the population of des-[30−75] correlates with an increase in the level of secondary structure.

Figure 3E shows the time dependence of the CD signal at 205 nm, indicating the formation of secondary structure. At this wavelength, a folded protein with secondary structure has a positive value but a protein with no secondary structure has a negative value.[15] Two control spectra of folded and unfolded protein have MRE (mean residue ellipticity) values of 1×10^3 and -9×10^3, respectively. Therefore, any increase in the magnitude of the CD signal at this wavelength shows the formation of secondary structure. As one can see in Figure 3E, this increase in the magnitude of the signal at 205 nm occurs over the same time scale in which unstructured ensemble $3S_U$ is not allowed to undergo S−S/SH reshuffling at pH 3. Therefore, this increase is the result of accumulation of secondary structure. The formation of secondary structure is slow enough to obtain structural information about the distribution of disulfide-bonded species at discrete times, which correspond to different stages in this folding transition. The initial formation of native-like structure in des-[30−75] can be observed 180 s into the transition, while details of the further stabilization of des-[30−75] can be studied further into the transition. The discrepancy between the initial signal of the kinetic trace (●) and the fully unfolded signal (○) is the result of a dead time of ∼2 min to mix the $3S_U$ stock solution in the appropriate buffer and prepare the anaerobic cuvette prior to the acquisition of data. This dead time is not an issue when preparing samples for NMR analysis because all of the preparation is performed at pH 3, a condition under which there is no folding progress. The decrease in pH is essentially instantaneous on the folding time scale (<1 s) so that the time during the transition to which the NMR spectra correspond is known accurately. According to the CD spectrum in Figure 3E, the MRE signal remains relatively constant from 1040 to 1800 s. This indicates that an equilibrium distribution is being attained between structured and unstructured species formed during this transition, which is consistent with the previous analysis by RP-HPLC. Consequently, the kinetic trace does not fully reach the purely folded signal (▼) because of the negative contribution of the unfolded signal at this time. Therefore, analysis of the progress 1200 s into this transition could identify the residues responsible for a stable distribution of three-disulfide-bonded species dominated by des-[30−75]. ^{1}H−^{15}N HSQC spectra were recorded at 180 and 1200 s to identify the residues involved in these two stages along the transition.

Analysis by NMR Spectroscopy of the $3S_U$-to-$3S_F$ Transition of ^{15}N-Enriched ONC. The ^{1}H−^{15}N HSQC spectrum of the $3S_U$ ensemble (Figure 4A) illustrates the characteristics of an unstructured protein with little chemical shift dispersion. The corresponding spectrum of native ONC (Figure 4B) illustrates the characteristic chemical shift dispersion of a structured protein. Both samples were subjected to a pulse of D_2O to decrease the contribution of the unstructured residues, although residual peaks from unstructured residues can be observed in Figure 4A due to back exchange of protons with remaining H_2O. The ^{1}H−^{15}N HSQC spectra of native ONC and the unstructured ensemble of $3S_U$ were used to identify amide hydrogens that are stabilized 180 and 1200 s into the $3S_U$-to-$3S_F$ transition, because there is a mixture of structured and unstructured species at these two times.

Panels A and B of Figure 5 show ^{1}H−^{15}N HSQC spectra of samples for which the $3S_U$-to-$3S_F$ transition was arrested at 180 and 1200 s, respectively. Figure 5A shows six (circled) resonances arising from structured regions; i.e., they overlap with resonances observed in native ONC (Figure 4B). These six resonances appear outside the region of the spectrum of Figure 4A that is associated with unfolded species. Additional resonances in Figure 5B, including those circled in Figure 5A, correspond to the spectrum of the native protein shown in Figure 4B. The regions containing these resonances are circled in Figure 5B.

Figure 6 shows four regions of the superposition of ^{1}H−^{15}N HSQC spectra of Figures 4B (green, native), 5A

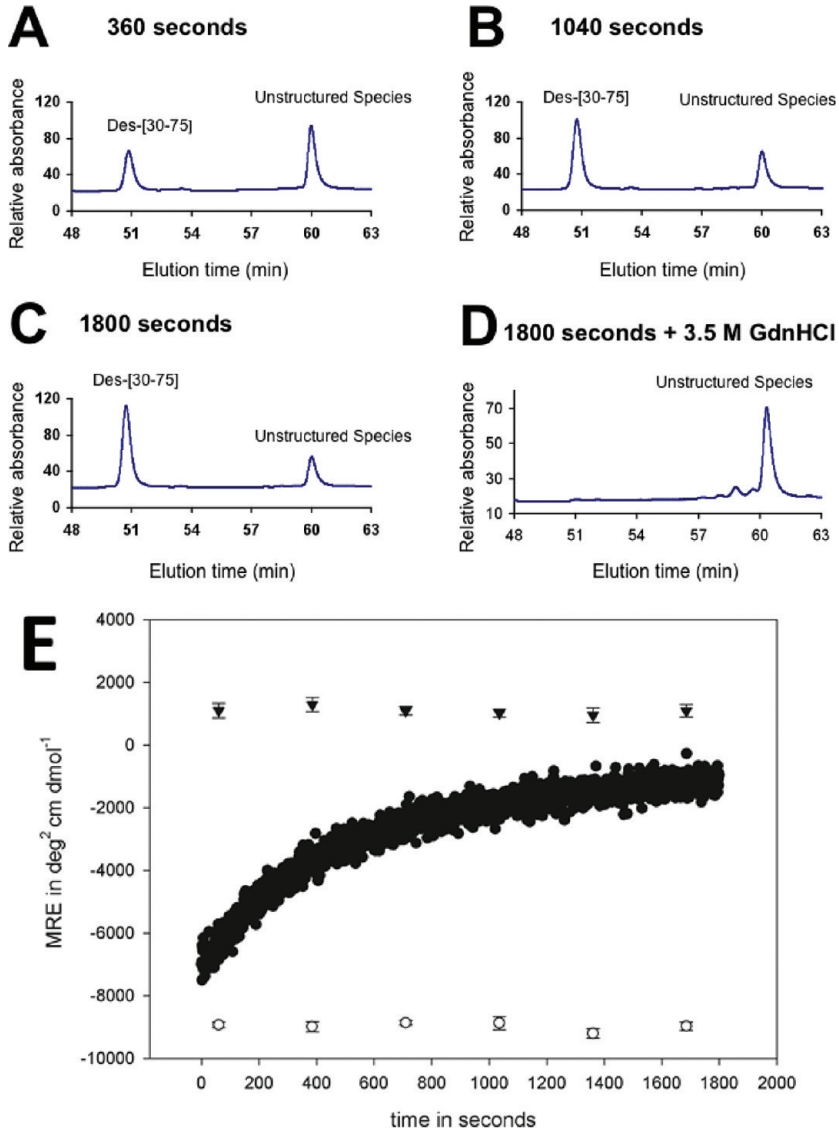

Figure 3. (A–C) RP-HPLC analysis of the distribution of structured and unstructured species after a reduction pulse to reduce the disulfide bonds of unstructured species yet keep disulfide bonds of structured species intact after 360 (A), 1040 (B), and 1800 s (C) is shown in the top panels. As the amount of secondary structure increases, indicated by CD, the concentration of des-[30–75] also increases, indicated by the RP-HPLC diagrams, as a result of an increasing number of native interactions. The identical distribution of species in panels B and C indicates that a stable distribution is formed 1040 s into this transition. The initial addition of GdnHCl before starting the $3S_U$-to-$3S_F$ transition prevents native interactions from forming, and consequently, des-[30–75] does not appear (D). (E) Kinetic trace of the $3S_U$-to-$3S_F$ transition of ONC, monitored by CD spectroscopy at 205 nm, pH 8.0, and 25 °C. The increase in the MRE (●) indicates an increase in the level of secondary structure. A CD spectrum of an unfolded protein has a negative signal at 205 nm. The CD signal from an unfolded protein (○) comes from the unstructured $3S_U$ ensemble at pH 3, a condition that does not allow S–S/SH reshuffling, and consequently, there is no progress in the $3S_U$-to-$3S_F$ transition. However, the signal from proteins with secondary structure would be positive. The CD signal from a folded protein (▼) comes from des-[30–75] at pH 3. The error bars from the folded and unfolded signals come from the standard deviation from averaging the signal for 2 s. A stable positive signal is observed 1040 s into this transition. $^1H-^{15}N$ HSQC spectra were recorded 180 and 1200 s into the $3S_U$-to-$3S_F$ transition to identify the initial and later nativelike structure formed, respectively.

(red, acquired after 180 s), and 5B (purple, acquired after 1200 s). Panels A–D show different regions of the $^1H-^{15}N$ HSQC spectra. In all of the panels of Figure 6, the purple (1200 s) and red (180 s) resonances are superposed on the green resonances of the spectrum of the native protein, which indicates that the corresponding residues are involved in nativelike structure. In the regions shown in Figure 6, no resonances from the spectra of the unfolded protein (Figure 4A) are superimposed onto resonances from the native spectrum, or on the 180 and 1200 s spectra, indicating that these resonances correspond to amide protons of a folded protein.

Figure 7 shows the intensities of the peaks in the $^1H-^{15}N$ HSQC spectra of panels A and B of Figure 5 corresponding to the residues listed in Tables 1 and 2, respectively. The relative intensities of the peaks at 180 and 1200 s suggest that some regions of ONC are stabilized at 180 s while other regions show native structure only at 1200 s. Six peaks (Table 1) exhibit chemical shifts corresponding to the native structure at 180 s, whereas 37 peaks (Table 2) exhibit chemical shifts consistent with native structure at 1200 s. One possibility is that, rather than representing an intermediate structure, the six peaks observed at 180 s arise from des-[30–75] and are merely the

dx.doi.org/10.1021/bi201168d | *Biochemistry* 2012, 51, 521–532

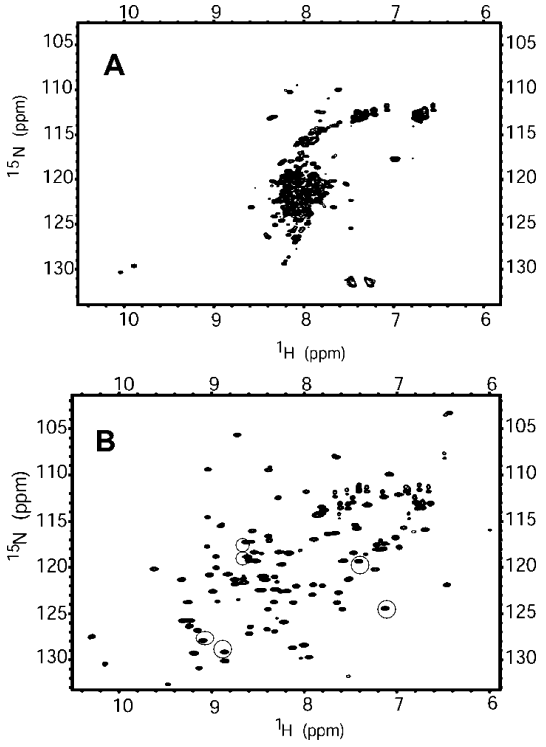

Figure 4. (A) ^{1}H−^{15}N HSQC spectrum of the $3S_U$ ensemble prepared as described in the legend of Figure 2B without allowing the $3S_U$-to-$3S_F$ transition to proceed. The close localization of the peaks is indicative of an unfolded protein. (B) ^{1}H−^{15}N HSQC spectrum of native ONC prepared as described in Figure 2A. The native structure gives rise to diverse chemical environments for the amide hydrogens as indicated by the distribution of the peaks in this spectrum. The circled resonances are observed in Figure 5A, which identifies the initial nativelike structure observed in this transition.

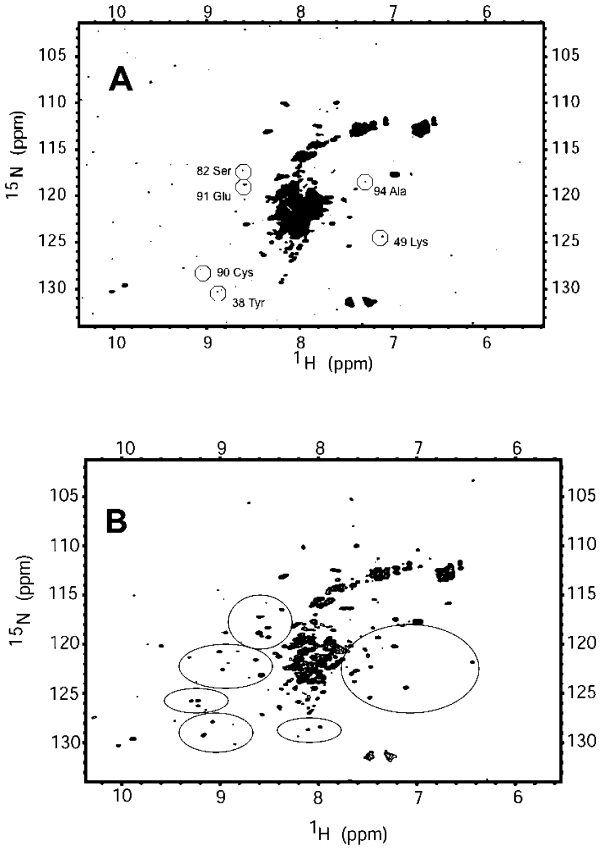

Figure 5. (A) ^{1}H−^{15}N HSQC spectrum of the folding transition 180 s into the $3S_U$-to-$3S_F$ transition. More resonances are observed outside the unfolded region observed in Figure 4A. The circled resonances are not observed in Figure 4A. These resonances are also circled in Figure 4B. (B) ^{1}H−^{15}N HSQC spectrum taken 1200 s into the $3S_U$-to-$3S_F$ transition. The circled regions in this panel indicate resonances that are found in Figure 4B. The presence of these peaks indicates the formation of nativelike structure during this transition.

most intense in the spectrum. However, this is probably not the case because these six peaks, observed at 1200 s, are not the most intense in the spectrum and have intensities similar to those of the 31 remaining peaks. This suggests that an intermediate is populated at 180 s but a significant amount of des-[30−75] is observed at 1200 s, and that the intermediate structure is populated in regions that are stabilized more efficiently.

Because the observed amide protons belonging to stabilized residues have the same chemical shifts as those found in the spectrum of the native protein, and thus the same chemical environment, the interactions displayed in the crystal structure that show contacts with these amide protons can be identified as those that are involved in the initial formation of nativelike structure during this transition. The NMR-derived structure[14] agrees with the crystal structure with a root-mean-square deviation (rmsd) of 0.74 Å. These contacts would include hydrogen bonding partners to the amide hydrogens as well as other atoms from side chains of neighboring residues. Tables 1 and 2 list the residues that contain amide protons that are involved in nativelike structure after 180 and 1200 s, respectively. The hydrogen bonding partner for each amide proton, namely, the carbonyl oxygen of a neighboring residue, as well as the secondary structure element that contains this hydrogen bond are also listed. Figure 8 shows the location of these amide protons 180 and 1200 s into the $3S_U$-to-$3S_F$ transition, as well as the four disulfide bonds in ONC.

Structure Stabilized at 180 s. Three of the residues listed in Table 1, stabilized 180 s into the $3S_U$-to- $3S_F$ transition, are in the vicinity of the C-terminus of the protein and are involved in a loop consisting of residues 90−94, namely, Cys90, Glu91, and Ala94 (Figure 8A,B). These residues form complementary hydrogen bonds leading to antiparallel β-strands. Glu91 and Ala94 are involved in two hydrogen bonds with each other, where the amide proton of Glu91 is hydrogen bonded to the carbonyl oxygen of Ala94 and the amide proton of Ala94 is hydrogen bonded to the carbonyl oxygen of Glu91 (Figure 9A). These two residues close the four-residue loop (Glu91-Asn92-Gln93-Ala94) in this β-strand. While the amide proton of Cys90 is not involved in the hydrogen bonding of this strand, interactions with the side chain of the neighboring residue, Thr89, presumably help stabilize the hydrogen bond between the amide proton of Cys90 and the carbonyl oxygen of Lys55 (Figure 9B). Also, because this loop is in the proximity of the 48−90 disulfide bond, this structural element could very likely protect the 48−90 disulfide bond from S−S/SH interchange.

Of all the loop motifs in this protein, this four-residue loop motif is the shortest. Therefore, formation of these hydrogen bonds involves the smallest entropic penalty in loop closure. Thus, it is especially favorable for these hydrogen bonds to form early in the folding process to initiate formation of this loop. This motif brings Cys87 and Cys104 into the proximity of each other to form a disulfide bond (Figure 8 E,F), which is

dx.doi.org/10.1021/bi201168d | *Biochemistry* 2012, 51, 521−532

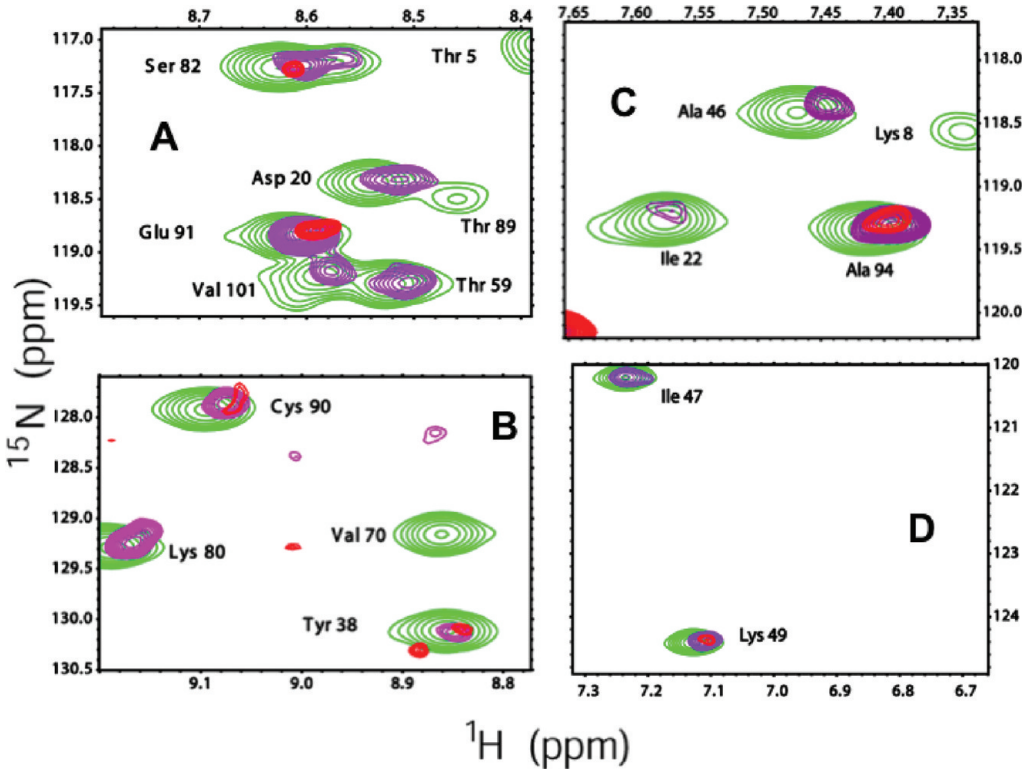

Figure 6. Superposed ^{1}H−^{15}N HSQC spectra from different regions of panels A and B of Figure 4 and panels A and B of Figure 5 used to identify resonances that indicate the initial formation of structure. The green resonances are from Figure 4B, which correspond to the native structure. The purple resonances are from Figure 5B, which correspond to spectra acquired after 1200 s. The red resonances are from Figure 5A, which correspond to spectra acquired after 180 s. No resonances from the unfolded spectrum of Figure 4A are superposed on these resonances, indicating that these resonances correspond to amide hydrogens of structured species.

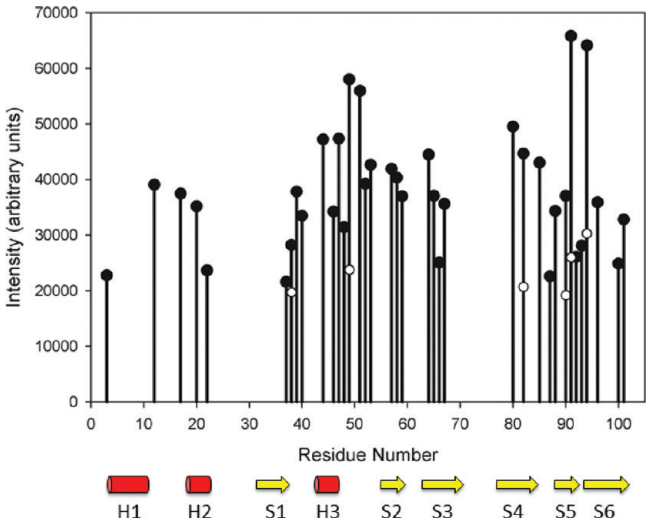

Figure 7. Plot of the intensities of resonances detected in the ^{1}H−^{15}N HSQC spectra of panels A and B of Figure 5 that indicate an intermediate with chemical shifts similar to those of the nativelike structure at the corresponding residue numbers, which are listed in Tables 1 and 2. Resonances detected 180 s into the $3S_U$-to-$3S_F$ transition are shown as empty circles and those detected after 1200 s as filled circles. The noise level for each of the spectra is 4.5×10^3. The elements of secondary structure, of which each residue is a part, are listed below and are numbered according to Figure 1. Helices are denoted with an H and are represented as red cylinders. Strands are denoted with an S and are represented as yellow arrows.

formed in the first structured intermediate in the oxidative folding pathway, des-[19−68, 30−75].

Table 1. Residues[a] that Contain Amide Protons Identified from Resonances Observed in a ^{1}H−^{15}N HSQC Spectrum Taken 180 s into the $3S_U$-to-$3S_F$ Transition and are Indicative of Nativelike Structure[b]

amide proton[a]	carbonyl oxygen[c]	structural element[d]
Tyr38	Tyr64	loop 4
Lys49	Ala46	loop 5
Ser82	Leu65	strand 4
Cys90	Lys55	strand 5
Glu91	Ala94	loop 9
Ala94	Glu91	loop 9

[a]Hydrogen bond donors. [b]The numbered loops and strands refer to Figure 1. [c]Hydrogen bond acceptors chosen by assuming native structure (PDB entry 1ONC). [d]Secondary structure element that contains the hydrogen bond to the residue in the left column, also by assuming native structure.

Hydrophobic interactions are presumably responsible for stabilizing nativelike structure surrounding the hydrogen bond between the amide hydrogen of Lys49 and the carbonyl oxygen of Ala46. The hydrophobic methylenes of the side chain of Lys45 contact the two ring CH_2 groups of Pro95 and the CH_3 group of Ala94 (Figure 9C) and help shield the amide proton of Lys49 from H/D exchange. Also, this contact is in the vicinity of the 48−90 disulfide bond and would presumably help stabilize it from S−S/SH interchange. The stabilization of the 48−90 disulfide bond early in the folding pathway is consistent with the fact that the 48−90 disulfide bond is also formed in the first structured species, des-[19−68, 30−75], in the oxidative folding pathway.

dx.doi.org/10.1021/bi201168d | *Biochemistry* 2012, 51, 521−532

Table 2. Detectable Amide Protons Involved in Nativelike Structure after 1200 s, As Seen in a $^{1}H-^{15}N$ HSQC Spectrum

amide proton[a]	carbonyl oxygen[b]	structural element[c]
Trp3		loop 1
Thr12	Ile37	loop 2
Val17	Arg15	loop 2
Asp20		helix 2
Ile22	Arg18	helix 2
Ile37	His10	sheet 1
Tyr38	Tyr64	loop 4
Ser39	Thr12	loop 4
Arg40		loop 4
Val44	Arg40	helix 3
Ala46	Glu42	helix 3
Ile47	Val44	helix 3
Cys48	Lys45	helix 3
Lys49	Ala46	loop 5
Ile51	Cys48	loop 5
Ile52	Gly50	loop 5
Ala53		loop 5
Val57	Val88	strand 2
Leu58		loop 6
Thr59	Phe86	loop 6
Tyr64	Tyr38	strand 3
Leu65	Ser82	strand 3
Ser66	Phe36	strand 3
Asp67	Lys80	strand 3
Lys80	Asp67	strand 4
Ser82	Leu65	strand 4
Lys85		loop 8
Cys87	Gly100	strand 5
Val88	Val57	strand 5
Cys90	Lys55	strand 5
Glu91	Ala94	loop 9
Asn92	Ile52	loop 9
Gln93	Ile51	loop 9
Ala94	Glu91	loop 9
Val96	Thr89	strand 6
Gly100	Cys87	strand 6
Val101		loop 10

[a]Amide protons that adopt nativelike structure after 180 s are also observed after 1200 s. [b]Hydrogen bond acceptors chosen by assuming native structure (PDB entry 1ONC). [c]Secondary structure element, labeled in Figure 1, that contains this hydrogen bond to the residues in the left column, also by assuming native structure.

While Tyr38 and Ser82 are separated by many residues in the amino acid sequence, nativelike structure in the vicinity of these amide hydrogens is formed by hydrophobic contacts with the side chain of Arg15 after 180 s (Figure 9D). Tyr38 and Ser82 are involved in hydrogen bonds with Tyr64 and Leu65, respectively, in the crystal structure. These two hydrogen bonds are not in the vicinity of disulfide bonds, in contrast to the other four residues listed in the left column of Table 1. Therefore, they must be stabilized by interactions with the neighboring side chains of Arg15, Tyr38, Tyr65, and Lys81. The guanidino group of Arg15 contacts the amide hydrogen of Ser82. This contact would presumably be stabilized by additional contacts of the hydrophobic methylenes of the side chain of Arg15 observed in the crystal structure with the aromatic rings in the side chains of Tyr38 and Tyr65. In addition, the hydrophobic methylenes in the side chain of Lys81 also contact the aliphatic carbons of the side chain of Arg15.

Structure Stabilized after 1200 s. Those interactions formed after 180 s provide a scaffold for additional native structure that is stabilized after 1200 s. The amide protons observed after 1200 s are listed in Table 2. Further structure includes a loop containing Asn92 and Gln93, which allows additional hydrogen bonds to form in the antiparallel β-sheet consisting of residues 87−100 and, further, stabilizes the 87−104 disulfide bond (Figure 8E,F). Another structural element that is stabilized after 1200 s is the loop containing residues 49−55. The carbonyl oxygens of Ile51 and Ile52 of this loop form hydrogen bonds with the amide hydrogen atoms of the loop containing Gln93 and Asn92, respectively (Figure 8C,D), with mutual cooperating stabilization of these two loops and the disulfide bond between Cys48 and Cys90. After 1200 s, the interactions in the vicinity of the side chain of Arg15 initialize the formation of the three-stranded antiparallel β-sheet in the core structure of the protein consisting of residues 34−37, 64−69, and 78−83.

The stabilization of the secondary structure elements listed in Table 2 shows how the des-[30−75] species is selectively populated along the $3S_U$-to-$3S_F$ transition. According to Table 2, there are no resonances in the vicinity of the disulfide bond, 30−75, colored yellow in panels E and F of Figure 8, which indicates that this disulfide bond is not formed in 1200 s. The observation that no residues in the vicinity of Cys30 and Cys75 have stabilized protons is consistent with the RP-HPLC analysis of this transition that found that no disulfide is formed between residues Cys30 and Cys75. In other words, thermodynamically favorable interactions involving the side chains of non-cysteine residues are presumably responsible for the stabilization of des-[30−75] rather than any from the addition of a disulfide bond.

DISCUSSION

The formation of the oxidative folding intermediate, des-[30−75] of ONC, through S−S/SH reshuffling at pH 8.0 without oxidation to the four-disulfide form, from an ensemble of unstructured three-disulfide species that contain native and nonnative disulfide bonds was examined. The native disulfide bond connectivity of des-[30−75] results from thermodynamically favorable interactions. Because the increase in the concentration of des-[30−75] by S−S/SH reshuffling could be arrested at different times by lowering the pH to 3, the stabilized portions of the protein during the $3S_U$-to-$3S_F$ transition were identified (Figure 8). $^{1}H-^{15}N$ HSQC spectra, collected at different times, identified amide protons of stabilized residues with chemical shifts found in the spectrum of native ONC, which had been assigned previously.[14] From these interactions, folding events in the initial formation of nativelike structure have been identified.

Comparison with Previous Research on RNase A and ONC. Previous NMR studies of three-disulfide-bond-containing oxidative folding intermediates of RNase A, des-[65−72] and des-[40−95],[12,16] are consistent with the NMR experiments performed on des-[30−75] of ONC in this study, in the sense that these intermediates of RNase A have nativelike structure except in the vicinity of the 65−72 and 40−95 disulfide bonds, respectively. Residues in the vicinity of these missing disulfide bonds in RNase A have substantial differences in chemical shifts versus those in the wild-type protein and experience an increased rate of H/D exchange.[12,16] Similarly, with des-[30−75] of ONC, a substantial number of resonances in the $^{1}H-^{15}N$ HSQC spectra of des-[30−75] correspond to resonances in the spectrum of

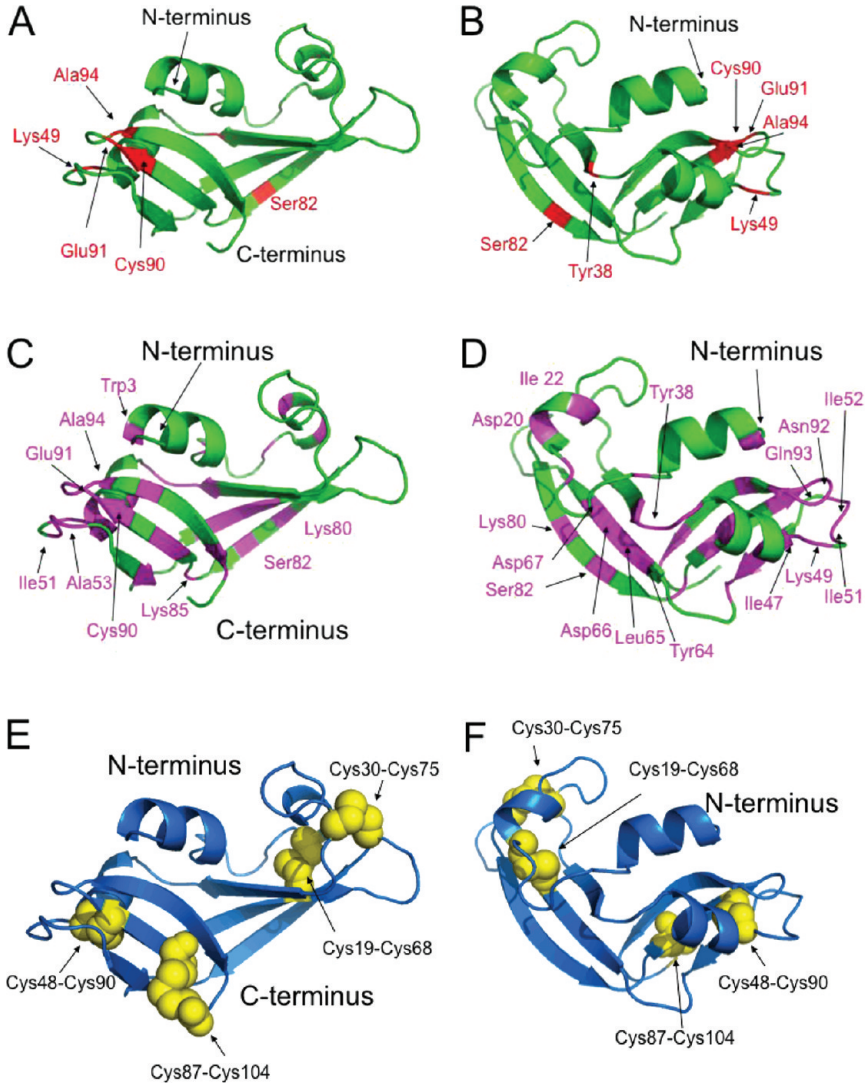

Figure 8. X-ray structure of ONC (PDB entry 1ONC). (A and B) Views of ONC that show, in red, the residues that contain stabilized amide protons 180 s into the $3S_U$-to-$3S_F$ transition. (C and D) Views of the same position as panels A and B, respectively, which show stabilized amide protons not only after 180 s but also after 1200 s (purple). (E and F) Disulfide bonds in ONC in space-filled spheres in positions identical to those in panels C and D, respectively.

native ONC, and no resonances that correspond to residues in the vicinity of the 30−75 disulfide bond are observed.

In an earlier study of the disulfide-bond-intact folding pathway of guanidine-denatured ONC, quench-flow methods coupled with H/D exchange and two-dimensional NMR spectroscopy identified 31 amide hydrogens of stabilized residues from the protein backbone as the earliest detectable structure in ONC after 250 ms, and folding was complete in ~5 s.[17] Because folding was so rapid in this study,[17] it was not possible to obtain much detail about early folding events. By contrast, in our oxidative folding study, by allowing S−S/SH interchange to occur along the $3S_U$-to-$3S_F$ transition, we found the formation of native structure occurs on a much longer time scale, 1200 s. This made it possible to detect the first six amide hydrogens to be involved in nativelike structure after 180 s. Almost all of the amide hydrogens of residues stabilized after 1200 s are the same as those first detected in the previous work.[17] Therefore, these experiments have allowed us to study much earlier events in the folding of onconase. The formation of secondary structure monitored by H/D exchange and mass spectroscopy on a longer time scale during disulfide-dependent folding has also been observed in an all-α-helical protein.[18] In that study, intermediates with different numbers of disulfide bonds were isolated from the oxidative folding of LR^{3}IGF-I. As the number of disulfide bonds increased in each intermediate, less H/D exchange occurred, which is indicative of an increasing level of secondary structure. Therefore, slow folding behavior is not restricted to ONC or other proteins that have β-sheets, and the interactions discussed below can be applicable to folding events in other proteins.

Comparison between the Structure Stabilized after 180 s and Chain Folding Initiation (CFI) Site in RNase A

The observation of early folding events in ONC after 180 s has allowed us to compare the mechanism of formation of chain-folding initiation (CFI) sites in ONC to those of proposed structurally homologous CFI sites in RNase A. Of special interest is the strand−loop−strand motif forming an antiparallel β-sheet consisting of residues 87−96 (CVTCENQAPV). This sheet in the C-terminal region of ONC is in a structurally homologous position to the C-terminal antiparallel β-sheet consisting of residues 106−118 (IIVACEGNPYVPV) in RNase A, which was proposed to be the CFI site, "F".[19,20]

dx.doi.org/10.1021/bi201168d | *Biochemistry* 2012, 51, 521−532

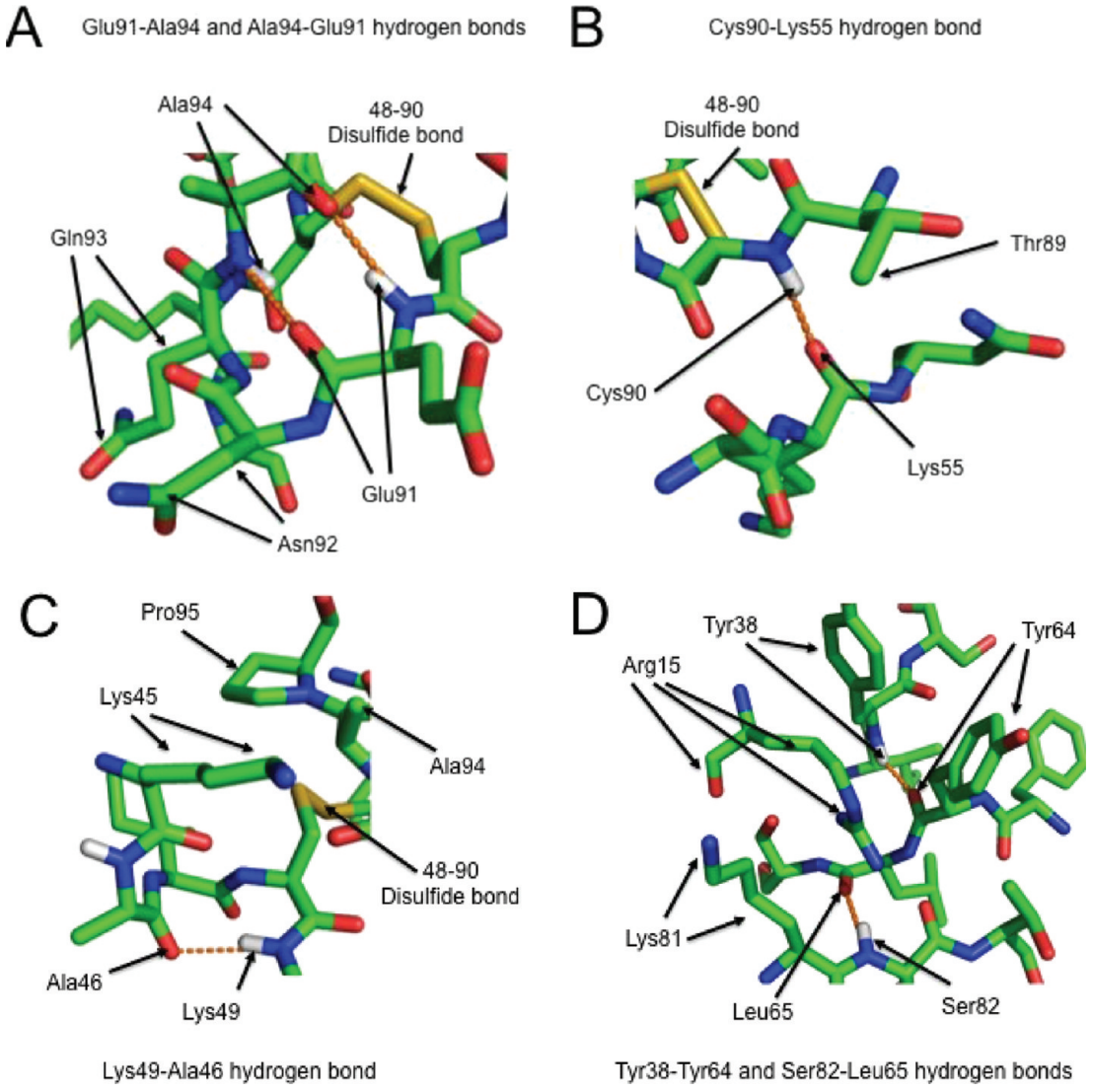

Figure 9. Contacts surrounding the hydrogen bonds that contain the amide protons of residues detected 180 s into the transition and involved in nativelike structure (PDB entry 1ONC). Showing the van der Waals radii of the atoms would bring out the packing of these contacts more clearly but, at the same time, would complicate the view of the hydrogen bonds. To show the orientation of the residues surrounding the hydrogen bonds, the structures are represented as stick models. Carbon atoms are colored green, nitrogen atoms blue, hydrogen atoms white, oxygen atoms red, and sulfur atoms yellow. Hydrogen bonds are represented as dotted orange lines. The residues that flank the donors and acceptors of the hydrogen bonds in the amino acid sequence are also shown. (A) The complementary hydrogen bonds between Glu91 and Ala94 close the shortest loop region (Glu91-Asn92-Gln93-Ala94) in ONC. This structural element presumably helps shield the 48−90 disulfide bond, indicated by an arrow, from S−S/SH reshuffling. (B) The side chain CH_3 group of Thr89, which contacts the amide proton of Cys90, presumably stabilizes the hydrogen bond between the amide proton of Cys90 and the carbonyl oxygen of Lys55. (C) The contacts between two ring CH_2 groups of Pro95, the CH_3 group of Ala94, and the hydrophobic methylenes in the side chain of Lys45 presumably stabilize the hydrogen bond between Lys49 and Ala46. Also, these contacts are in the vicinity of the 48−90 disulfide bond, indicated by an arrow, and, as a result, would stabilize this disulfide bond by preventing S−S/SH reshuffling. (D) The guanidino group of Arg15, indicated by an arrow, is in the vicinity of the amide proton of Ser82. The guanidino group is presumably oriented by hydrophobic contacts between the aromatic rings of Tyr38 and Tyr64, and the hydrophobic methylenes in the side chain of Lys81 and the methylenes of the side chain of Arg15, all indicated by arrows. The hydrophobic contacts involving the side chains of Arg15, Lys81, Tyr38, and Tyr64 would stabilize the hydrogen bonds between the amide proton of Tyr38 and the carbonyl oxygen of Tyr64 as well as between the amide proton of Ser82 and the carbonyl oxygen of Leu65.

Hydrophobic interactions among nonpolar residues, Ile106, Ile107, Val108, Val116, and Val118, of RNase A bring the strands together to form a loop. ONC does not contain a similar number of nonpolar residues in this motif and must use other interactions, such as the hydrogen bonds involving the 91−94 loop, to stabilize it. Another difference between these motifs is that there are six loop residues (EGNPYV) within the CFI site in RNase A while there are four loop residues in ONC (ENQA). We found that the 91−94 loop region in ONC is stabilized by hydrogen bonds between residues Glu91 and Ala94 in the C-terminal antiparallel β-sheet of ONC after 180 s, and that this sheet is stabilized further after 1200 s. This suggests that, in this sheet in ONC, the loop region is stabilized first, before interstrand hydrogen bonds are formed, which is a pathway different from that in RNase A for stabilizing this antiparallel β-sheet; i.e., hydrophobic interactions that initiate the folding of these β-strands in RNase A are farther from the loop region in this antiparallel β-sheet than in ONC.

dx.doi.org/10.1021/bi201168d | *Biochemistry* 2012, 51, 521−532

Hydrophobic interactions play a role in stabilizing a region in ONC structurally homologous to the CFI site, "E", of RNase A. This site in RNase A is comprised of residues 71−90 and 91−111, which form a β-sheet in the core of the protein. Strands 3 and 4 in ONC form a similar β-sheet. The interactions between the aliphatic carbons in the side chain of Arg15 and the aromatic rings in the side chains of Tyr38 and Tyr64 as well as the interactions between the guanidino group in the side chain of Arg15 and the aliphatic carbons in the side chain of Lys81 in ONC (Figure 9) bring strands 3 and 4 together in 180 s, with further stabilization provided after 1200 s. In addition, loop 4, which contains Tyr38, is also initially stabilized by this interaction. Similar hydrophobic packing that spans these strands is not found in the structurally homologous region in RNase A. Therefore, this mechanism for formation of this β-sheet in ONC is different from that in RNase A.

Hydrophobic interactions also bring together two regions in ONC that are structurally homologous to CFI sites D and F in RNase A. The two ring CH_2 groups of Pro95 and the CH_3 group of Ala94 of strand 6 interact with the hydrophobic methylenes in the side chain of Lys45 of helix 3 to bring these two structural elements together. Helix 3 in ONC is part of the structurally homologous region in CFI site D in RNase A, which is comprised of residues 53−79 in RNase A, and strand 6 in ONC is part of the structurally homolgous CFI site F in RNase A, which is comprised of residues 106−118. Ala94 is part of a loop region (Glu91-Asn92-Gln93-Ala91) that is stabilized 180 s into the transition. Bringing two regions of ONC that adopt nativelike structure into the proximity of each other early in the folding process helps ONC adopt native structure efficiently.

CONCLUSIONS

$^1H-^{15}N$ HSQC spectra acquired at different stages of the $3S_U$-to-$3S_F$ transition identified backbone amide protons that are involved in the initial formation of nativelike structure. By identification of the backbone amide protons of stabilized residues at different stages in the folding process that are involved in forming the initial nativelike structure, initial folding events of an unfolded state have been identified.

Favorable hydrogen bond interactions between two residues (Glu91 and Ala94) in a short loop and favorable interactions with nonpolar groups on side chains, e.g., Arg15 with Tyr38, Ser82 and Lys81, and Lys45 with Pro95 and Ala94 in long loops stabilize six amide hydrogens (Table 1 and Figure 9). These long loops could be formed because they contain favorable interactions that offset the larger entropic penalty to close them, compared to the smaller entropic penalty involved in closing a shorter loop. By observing the formation of these loops very early in the protein folding pathway, we found these favorable interactions illustrate how transient structure can be present in partially unfolded proteins or how secondary structure, especially β-sheets, starts to form. In addition, by identifying these redox-independent interactions that are formed in the folding pathway, we gained insight into the events that are important in the successful recognition by quality control mechanisms in cells. If these interactions cannot form at a given oxidation potential in a cell, which is carefully regulated, the protein may misfold and be shuttled to a degradation pathway.[21]

AUTHOR INFORMATION

Corresponding Author

*Telephone: (607) 255-4034. Fax: (607) 254-4700. E-mail: has5@cornell.edu.

Funding

This work was supported by National Institutes of Health Grant GM-24893.

ACKNOWLEDGMENTS

We thank R. J. Youle for providing the plasmid for ONC and Professor Linda Nicholson and Jolita Seckute for their help in acquiring NMR spectra.

ABBREVIATIONS

ONC, onconase; nS_U, ensemble of unstructured n-disulfide bond species that contain a distribution of native and non-native disulfide bonds; $3S_F$, structured three-disulfide bond intermediate species all of whose disulfide bonds are native; des-[x−y], species that contains native disulfide bonds but lacks the x−y disulfide bond; HDX, hydrogen/deuterium exchange; RNase A, bovine pancreatic ribonuclease A; $^1H-^{15}N$ HSQC, heteronuclear single-quantum coherence between ^{15}N and ^1H atoms; RP-HPLC, reversed phase high-performance liquid chromatography; MRE, mean residue ellipticity; pH*, uncorrected pH reading of a D_2O buffer; GdnHCl, guanidinium hydrochloride; Tris, tris(hydroxymethyl)aminomethane hydrochloride; TFA, trifluoroacetic acid; DTT^{red}, reduced dithiothreitol; PDB, Protein Data Bank; TOCSY, total correlation spectroscopy; NOESY, nuclear Overhauser enhancement spectroscopy

REFERENCES

(1) Rothwarf, D. M., Li, Y.-J., and Scheraga, H. A. (1998) Regeneration of bovine pancreatic ribonuclease A: Detailed kinetic analysis of two independent folding pathways. *Biochemistry 37*, 3767−3776.

(2) Gahl, R. F., and Scheraga, H. A. (2009) Oxidative folding pathway of onconase, a ribonuclease homolog: Insight into oxidative folding mechanisms from a study of two homologs. *Biochemistry 48*, 2740−2751.

(3) Schmid, F. X., and Baldwin, R. L. (1979) Detection of an early intermediate in the folding of ribonuclease A by protection of amide protons against exchange. *J. Mol. Biol. 135*, 199−215.

(4) Houry, W. A., and Scheraga, H. A. (1996) Structure of a hydrophobically collapsed intermediate on the conformational folding pathway of ribonuclease A probed by hydrogen-deuterium exchange. *Biochemistry 35*, 11734−11746.

(5) Dempsey, C. E. (2001) Hydrogen exchange in peptides and proteins using NMR-spectroscopy. *Prog. Nucl. Magn. Reson. Spectrosc. 39*, 135−170.

(6) Oh, H., Breuker, K., Sze, S. K., Ge, Y., Carpenter, B. K., and McLafferty, F. W. (2002) Secondary and tertiary structures of gaseous protein ions characterized by electron capture dissociation mass spectrometry and photofragment spectroscopy. *Proc. Natl. Acad. Sci. U.S.A. 99*, 15683−15688.

(7) Li, X., Hood, R. J., Wedemeyer, W. J., and Watson, J. T. (2005) Characterization of peptide folding nuclei by hydrogen/deuterium exchange-mass spectrometry. *Protein Sci. 14*, 1922−1928.

(8) Uzawa, T., Nishimura, C., Akiyama, S., Ishimori, K., Takahashi, S., Dyson, H. J., and Wright, P. E. (2008) Hierarchical folding mechanism of apomyoglobin revealed by ultra-fast H/D exchange coupled with 2D NMR. *Proc. Natl. Acad. Sci. U.S.A. 105*, 13859−13864.

(9) Bédard, S., Mayne, L. C., Peterson, R. W., Wand, A. J., and Englander, S. W. (2008) The foldon substructure of staphylococcal nuclease. *J. Mol. Biol. 376*, 1142−1154.

(10) Gahl, R. F., Narayan, M., Xu, G., and Scheraga, H. A. (2008) Dissimilarity in the oxidative folding of onconase and ribonuclease A, two structural homologs. *Protein Eng., Des. Sel. 21*, 223−231.

(11) Xu, G., Narayan., Welker, E., and Scheraga, H. A. (2004) Characterization of the fast-forming intermediate, des-[30−75], in the reductive unfolding of onconase. *Biochemistry 43*, 3246−3254.
(12) Shimotakahara, S., Rios, C. B., Laity, J. H., Zimmerman, D. E., Scheraga, H. A., and Montelione, G. T. (1997) NMR structural analysis of an analog of an intermediate formed in the rate-determining step of one pathway in the oxidative folding of bovine pancreatic ribonuclease A: Automated analysis of ^{1}H, ^{13}C, and ^{15}N resonance assignments for wild-type and [C65S, C72S] mutant forms. *Biochemistry 36*, 6915−6929.
(13) Narayan, M., Xu, G., Ripoll, D. R., Zhai, H., Breuker, K., Wanjalla, C., Leung, H. J., Navon, A., Welker, E., McLafferty, F. W., and Scheraga, H. A. (2004) Dissimilarity in the reductive unfolding pathways of two ribonuclease homologues. *J. Mol. Biol. 338*, 795−809.
(14) Gorbatyuk, V. Y., Tsai, C. K., Chang, C. E., and Huang, T. H. (2004) Effect of N-terminal and Met23 mutations on the structure and dynamics of onconase. *J. Biol. Chem. 279*, 5772−5780.
(15) Kelly, S. M., Jess, T. J., and Price, N. C. (2005) How to study proteins by circular dichroism. *Biochim. Biophys. Acta 1751*, 119−139.
(16) Laity, J. H., Lester, C. C., Shimotakahara, S., Zimmerman, D. E., Montelione, G. T., and Scheraga, H. A. (1997) Structural characterization of an analog of the major rate-determining disulfide folding intermediate of bovine pancreatic ribonuclease A. *Biochemistry 36*, 12683−12699.
(17) Schulenburg, C., Löw, C., Weninger, U., Mrestani-Klaus, C., Hofmann, H., Balbach, J., Ulbrich-Hofmann, R., and Arnold, U. (2009) The folding pathway of onconase is directed by a conserved intermediate. *Biochemistry 48*, 8449−8457.
(18) Li, X., Chou, Y.-T., Husain, R., and Watson, J. T. (2004) Integration of hydrogen/deuterium exchange and cyanylation-based methodology for conformational studies of cystinyl proteins. *Anal. Biochem. 331*, 130−137.
(19) Matheson, R. R. Jr., and Scheraga, H. A. (1978) A method for predicting nucleation sites for protein folding based on hydrophobic contacts. *Macromolecules 11*, 819−829.
(20) Montelione, G. T., and Scheraga, H. A. (1989) Formation of local structures in protein folding. *Acc. Chem. Res. 22*, 70−76.
(21) Ellgaard, L., Molinari, M., and Helenius, A. (1999) Setting the standards: Quality control in the secretory pathway. *Science 286*, 1882−1888.